# Electron-impact excitation and ionization of atomic calcium at intermediate energies

Oleg Zatsarinny, Henry Parker, and Klaus Bartschat

# Electron-impact excitation and ionization of atomic calcium at intermediate energies

Oleg Zatsarinny,* Henry Parker, and Klaus Bartschat

*Department of Physics and Astronomy, Drake University, Des Moines, Iowa, 50311, USA*

We present a comprehensive study of electron collisions with calcium atoms by using the convergent $B$-spline $R$-matrix method. Elastic, excitation, and ionization cross sections were obtained for all transitions between the lowest 39 physical states of calcium (except for $3p^6 4s5g$ $^{3,1}G$) up to the $3p^6 4s8s$ $^1S$ state, for incident electron energies ranging from threshold to 100 eV. A multi-configuration Hartree-Fock method with nonorthogonal term-dependent orbitals was employed to generate accurate wave functions for the target states. Close-coupling expansions including the 39 physical states plus 444 pseudo-target states of calcium were used to check the sensitivity of the results to coupling to the target continuum. The cross-section dataset obtained from the large-scale calculations is expected to be sufficiently accurate and comprehensive for most current modeling applications involving neutral calcium.

## I. INTRODUCTION

Accurate atomic data for electron collisions with atoms and ions are of importance in the modeling of a variety of astrophysical and laboratory plasmas. Electron-atom collisions couple the electron gas to the radiation field through atomic excitations and de-excitations, and thereby collision cross sections are crucial in determining the state of matter from the observed radiation field. This includes the investigation of the structure and evolution of galaxies, gas clouds, stars, and other objects that can be studied spectroscopically. Particular applications include stellar atmospheres, where large deviations from local thermal equilibrium (LTE) may be present. Abundance ratios allow the study of possible stellar nucleosynthesis mechanisms occurring in galaxies [1]. Having a set of NLTE calculations for various elements makes the comparison of the abundance ratios of the atomic species in different types of stars more reliable. Accuracy and completeness of the atomic data used is crucial in such modeling.

Calcium, one of the $\alpha$ elements, has observable lines along a broad range of wavelengths in late-type stellar spectra. The first detailed study of calcium lines in solar spectra was published by Holweger [2]. The presence of Ca lines in both solar and stellar spectra was confirmed in many subsequent papers. In particular, calcium lines were used for determinations of cool stellar atmospheric properties and for the study of chromospheric activity in late-type stars [3, 4]. Lines of both neutral and singly ionized Ca are observed even in most metal-poor stars [5] and can be used for the determination of fundamental stellar parameters.

Electron scattering from calcium has been the subject of a large body of research, both experimental and theoretical. Most of the studies, however, were devoted to elastic scattering and excitation of the resonance transi-

tion to the $4s4p$ $^1P^o$ state. A comprehensive discussion of elastic e-Ca collisions at low energies up to 4 eV is given in our previous paper [6]. In particular, comparison with other theoretical predictions revealed that the numerical results can be very model dependent. Comparison with various experimental data showed good agreement in some cases, while discrepancies remained in others. It was not immediately clear, however, whether these discrepancies were solely due to the omission of some important physics in the computational model or whether experimental problems might be responsible as well. The only experimental investigation of elastic e-Ca scattering at intermediate energies that we are aware of was carried out by Milisavljevic *et al.* [7]. Employing a crossed electron-atom beam technique, they measured the differential cross section (DCS) at incident energies of 10, 20, 40, 60 and 100 eV. Comparison with numerous theoretical investigations, performed mainly with various modifications of the optical model-potential (OMP) method, shows reasonably good agreement between the experimental and calculated DCSs concerning their angular dependence, whereas the agreement between the absolute values is not as good. The absolute values obtained theoretically are generally larger than those measured.

The cross section for the allowed transition $4s^2 - 4s4p$ $^1P^o$ is probably the most accurately known excitation cross section in Ca. Apparent cross sections for electron-impact excitation of this resonance transition were measured by Ehlers and Gallagher [8], whereas Milisavljevic *et al.* [9] obtained angle-differential cross sections for this transition for incident energies between 10 and 100 eV. This work prompted further theoretical efforts employing different methods and approaches. Chauhan *et al.* [10] used a first-order relativistic distorted-wave (RDW) model, whereas Kawazoe *et al.* [11] applied 15-state, 21-state, and 24-state nonrelativistic $R$-matrix (close-coupling) models to the problem. Later, Zatsarinny *et al.* [12] used the $B$-spline $R$-matrix (BSR) method to study electron-impact excitation of the lowest four excited states of calcium, and afterwards Fursa and Bray [13] applied the convergent

---
*Electronic Address: `oleg_zoi@yahoo.com`

close-coupling (CCC) method to the study of the $^1P^o$ excitation of Ca. These calculations with increasing level of sophistication improved the agreement with experiment. In particular, the CCC calculations revealed that models that neglect the coupling to the target continuum generally overestimate the cross section, even for this strong resonance transition.

The excitation of other states in Ca has been studied much less. Here we mention the joint theoretical and experimental work of Shafranyoshy *et al.* [14] devoted to the study of electron-impact excitation of Ca atoms from the metastable state $4s4p\,^3P^o$. The limited 6-state close-coupling calculations in this work did not achieve a comprehensive reproduction of the experimental data, but they were able to explain the principal features. Among other works, we note the RDW calculations by Muktavat *et al.* [15] concerning excitation of the low-lying $3d4s\,^{1,3}D$ states in Ca. These states, along with the strong exchange transition to the $4s4p\,^3P^o$ state, were also considered in our previous calculations [12], where considerable disagreement with the RDW results was found. To our knowledge, the only attempt to provide a systematic dataset for electron-impact excitation of Ca was undertaken by Samson and Berrington [16] who presented excitation cross sections and thermally averaged effective collision strengths for transitions from the $4s^2$ ground state to the next 10 states of Ca, based on a 22-state $R$-matrix model.

Plasma modelling requires a comprehensive set of data for transitions between all levels under consideration. The primary goal of the present work, therefore, is to provide a coherent and consistent set of data for electron collisions with Ca. From a fundamental point of view, it is also important to estimate the likely uncertainties of the available theoretical data. In addition to an accurate target representation, it is very important in this respect to check the convergence of the close-coupling expansion, particularly with respect to the contribution of the target continuum. Based on the CCC results for the $4s4p\,^1P^o$ excitation of Ca [13] and our previous calculations for Be [17] and Mg [18], we expected a strong influence of the target continuum, which has not yet been explored for Ca to full extent.

The present calculations were performed with the BSR method (for an overview, see [19]), employing an extended version of the associated computer code [20] that allows the inclusion of a sufficient number of physical target states as well as continuum pseudostates in the intermediate-energy regime. Our previous calculations [6, 12] contained only 39 physical target states. We therefore decided to extend these calculations using modern computing facilities by additionally including 444 continuum pseudostates. Using the same physical target states allows us to directly estimate the effect of coupling to the target continuum on the calculated excitation cross sections. Furthermore, the pseudostate approach also enables us to obtain ionization cross sections, thereby making the scattering data consistent, effectively complete,

and appropriate for plasma modelling. Note that the ionization cross sections in neutral Ca are still not well known. As discussed by Cvejanovic and Murray [21], there exists noticeable disagreement between various experimental data, both in the energy dependence and the magnitude at the cross-section maximum. Theoretically, single ionization of calcium by electron impact was so far only considered by perturbative methods. Consequently, it is interesting to explore whether the nonperturbative convergent pseudostate approach can help in resolving the existing discrepancies.

## II. COMPUTATIONAL METHODS

The target-structure and collision calculations in the present work were carried out in a similar manner to our previous calculations of electron scattering from calcium at low incident energies [6, 12]. Consequently, we will only summarize the specific features for the present case below, related to the pseudostate approach employed in the present calculations.

The target states of calcium were generated by combining the multi-configuration Hartree-Fock (MCHF) and the $B$-spline box-based close-coupling (CC) methods [22]. In this approach, the target wave functions for neutral Ca, $3p^64snl$, are expanded over the one-electron states of Ca$^+$, i.e., $3p^6nl$. Both valence and core-valence correlation are important for the ground state and the low-lying excited states of Ca. The core-valence correlations are included through the core-excited configurations in the CI expansions of the ionic states, whereas the valence correlations are accounted for through the mixing of different series $3p^6nln'l'$. Our final expansions include the $4snl$, $3dnl$, $4pnl$, $5snl$, $4dnl$, and $5pnl$ series. The unknown radial functions $P_{n\ell}$ for the outer valence electron were expanded in a $B$-spline basis, and the corresponding equations were solved subject to the condition that the wave functions vanish at the boundary. The $B$-spline coefficients for the valence orbitals $P_{n\ell}$ were obtained by diagonalizing the $N$-electron atomic Hamiltonian. This scheme leads to term-dependent valence orbitals, which are optimized individually for the states of interest. We also account for relaxation of the core orbitals caused by the deep core penetration of the $3d$ orbital.

An alternative and widely-used method of incorporating core-valence correlation is based upon applying a semi-empirical core-polarization potential (as was done, for example, in the CCC calculations [13]). Although such a potential simplifies the calculations significantly and can provide accurate excitation energies and oscillator strengths, the question always remains how well the model potential can simulate *all* core-valence correlation, including nonlocal and nondipole contributions. In the present approach, we therefore chose to include the core-valence correlation *ab initio* by adding target configurations with an excited core.

The number of spectroscopic bound states that can be

generated in the above scheme depends on the size $a$ of the $R$-matrix box. We included 140 $B$-splines of order 8 in the present calculations. Choosing $a = 80\,a_0$ (with $a_0 = 0.529 \times 10^{-10}$ m denoting the Bohr radius), we obtained a good description for all low-lying states of Ca up to $4s8s\ ^1S$, including some doubly-excited states of the $4p^2$ and $3d^2$. As discussed in [6], the above scheme provides a good target description regarding both the energy levels and the oscillator strengths. The deviations in the level energies from the recommended values [23] are generally less than 0.1 eV, except for the lowest $4s^2\ ^1S$ and $4s4p\ ^3P^o$ states, where the correlation corrections are expected to be most important. The accuracy of our binding energies is close to that achieved by extensive MCHF calculations [24], and the current structure description represents a substantial improvement over those used in previous $R$-matrix calculations. This is particularly noteworthy for the $3dnl$ states: directly including the core relaxation for these states drastically improves the corresponding binding energies.

The $B$-spline box-based close-coupling method is also able to generate continuum pseudostates that lie above the ionization threshold. The density and number of these states again depend on the box radius and, to a lesser extent, on other $B$-spline parameters, such as their order and distribution on the grid. The above approach is both a straightforward and general way to obtain the continuum pseudospectrum. It provides excellent flexibility by allowing us to vary the box radius or to change the density of the $B$-spline basis. As will be illustrated below, including the continuum pseudostates is extremely important to ensure the convergence of the final results for the excitation cross sections.

The scattering calculations were carried out by using a fully parallelized version of the BSR complex [20]. To check the influence of the target continuum, we set up two scattering models. The first model, labeled BSR-39, includes 39 physical target states, while the second model, labeled BSR-483, additionally contains 444 pseudostates that cover the target continuum up to 20 eV above the first ionization threshold. This model includes all target states with orbital angular momenta $L \le 4$, i.e., even $3p^64s5g\ ^{3,1}G$. This scattering model also allows us to obtain the ionization cross sections. The maximum number of scattering channels was 1,215. For a given $B$-spline basis, this number defines the size of the matrices involved, leading in the present case to generalized eigenvalue problems with matrix dimensions up to 150,000. Such large calculations require the use of supercomputers.

We calculated results for partial waves with total orbital angular momenta up to $L_{max} = 30$ numerically. Overall, with the various total spins and parities, this involved 124 partial waves. The calculation for the external region was performed with a parallelized version of the STGF program [25]. We considered all transitions between physical states, with the principal difficulty being the slow convergence of the partial-wave expansion for transitions between close-lying levels. When necessary
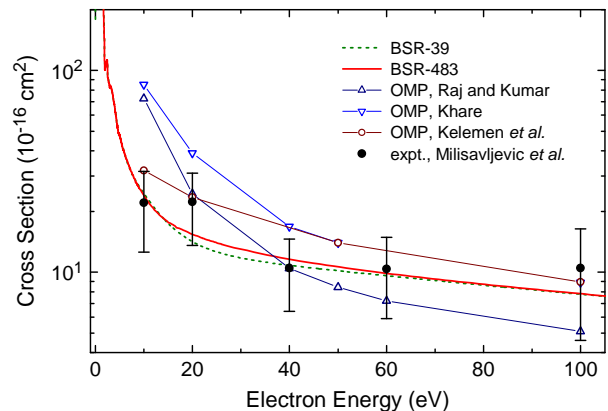


FIG. 1: Cross section for elastic electron scattering from calcium atoms at intermediate energies. The current BSR-39 and BSR-483 results are compared with OMP calculations of Khare *et al.* [27], Kelemen *et al.* [28], Raj and Kumar [29], and with measurements of Milisavljevic *et al.* [7].

we employed a top-up procedure based on the Coulomb-Bethe approximation [26].

## III. RESULTS

### A. Elastic cross sections

We begin the discussion of our results with elastic scattering from calcium, which is one of the most studied processes, both theoretically and experimentally. The angle-integrated elastic cross section at intermediate energies is given in Fig. 1. We see close agreement between the BSR predictions and the experimental data of Milisavljevic *et al.* [7] for all energies within the given error bars, except perhaps at except 20 eV, where the experimental value deviates from the expected smooth energy dependence of the elastic cross section. The small differences between the two sets of BSR results suggest that the effect of coupling to the target continuum for this process is very small, essentially negligible. Nevertheless, the good convergence in this case does not indicate that the calculations are trivial: for these energies there are many other calculations based on a variety of model potentials. They yield rather different results and agree with the measurements to a much lesser extent. We hence conclude that the nonperturbative R-matrix calculations are more reliable than previous predictions.

A comparison of angle-differential cross sections for elastic scattering is presented in Fig. 2. We obtain close agreement in both magnitude and angular dependence with the experimental DCS [7]. The good agreement between the BSR-39 and BSR-483 results indicates, once again, that coupling to the target continuum does not change the angular dependence significantly. The magnitude of the angle-integrated cross sections is almost completely determined by the small-angle region, up to
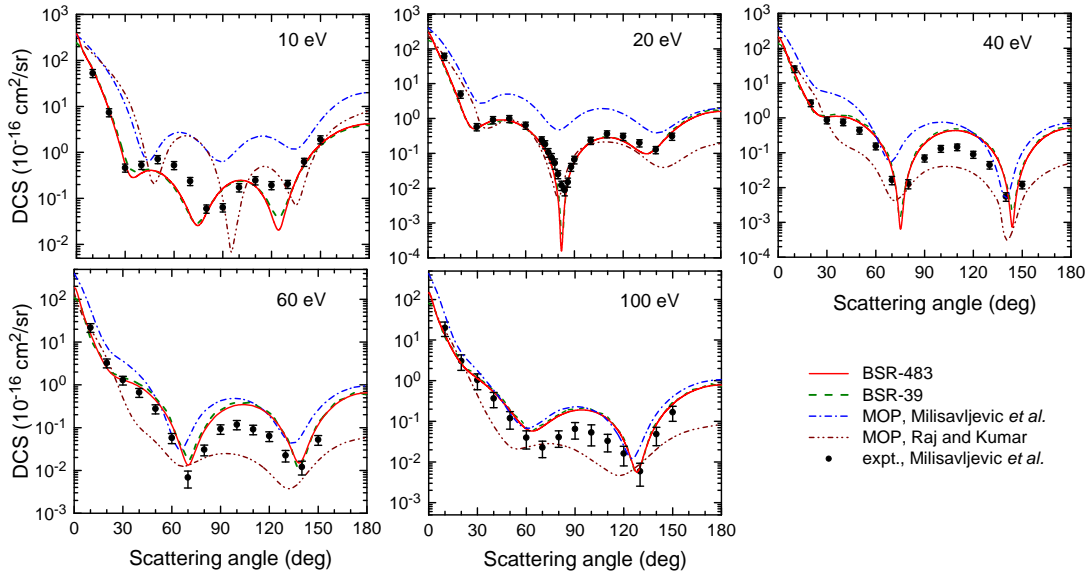
FIG. 2: Angle-differential cross sections for elastic electron scattering from calcium atoms for incident electron energies of 10, 20, 40, 60 and 100 eV. Our BSR results are compared with the experimental data of Milisavljevic *et al.* [7], as well as with OMP calculations from the latter work and the OMP results of Rai and Kumar [29].

20-25 degrees. The noticeable difference in the angle-integrated elastic cross sections at 20 eV, as discussed above, is mainly caused by the difference in the DCS values at 10 and 20 degrees. The absolute cross sections in [7] were obtained from the elastic-to-inelastic (to the resonant $4^1P^o$ state) intensity ratio at $\theta = 10$ degrees at each electron energy. As a result, the accuracy of the measurements for the DCSs for excitation directly affect the accuracy of the elastic DCS.

A comprehensive list of references and a discussion of earlier calculations for the elastic DCS was given by Milisavljevic *et al.* [7]. In Fig. 2 we compare only with a few somewhat recent calculations [7, 29], which all used a model-potential approach. This method provides a convenient and powerful tool for the quantum-mechanical treatment of electron scattering by atoms and molecules in the intermediate-energy region for complex atomic targets. It also offers a computationally simpler solution of the differential equation (effectively for potential scattering) than direct close-coupling approaches such as the *R*-matrix method used in the present work. Because of these features, the model-potential method continues to attract considerable interest. However, as seen from Figs. 1 and 2, the accuracy of this approach is severely limited.

The angular dependence of the elastic DCS at 10 eV exhibits three minima, at 30°, 70°, and 120°, respectively. As the energy increases, these minima move and change: the first minimum slowly transforms into a shoulder, the second moves towards smaller scattering angles, and the third becomes more pronounced. Generally, the calculated DCS curves show shapes similar to the experimental ones, except for the lowest energy of 10 eV where

the deviations are large. This is not surprising, since channel coupling should be most important at this energy. Also, the agreement with experiment regarding the absolute values is closest for the present *R*-matrix calculations. The optical potential used in [7] consists of the sum of static as well as local exchange and polarization potentials. The polarization potential contains a semi-empirical cut-off parameter, which was chosen to provide the best visual fit to the experimental DCS data at a particular energy. The authors concluded that the best agreement was obtained just with the static approximation while the static+exchange+polarization calculation generally gave larger DCS values.

Rai and Kumar [29] also used a model-potential approach, and one purpose of their work was to assess the contribution of absorption effects. Their optical potential was represented by an energy-dependent central, local and complex potential to simulate the static, exchange, polarization, absorption, and spin-orbit interaction effects. This calculation, which takes all the above-mentioned effects into account, represents the previously most comprehensive model potential for Ca atoms at intermediate energies.

As seen from Fig. 2, the level of agreement between the absolute values of the cross sections obtained by Rai and Kumar [29] and the experimental data varies depending on the incident energy and the scattering angle. The authors concluded that the large error bars call for more accurate measurements to draw meaningful conclusions about the agreement of the absolute DCS values obtained by theory and experiment. The good overall agreement of the measurement with the present *R*-matrix calculations, however, suggests that the measurement is

sufficiently accurate to represent all main features in the DCS for elastic e-Ca scattering and, together with the present results, can serve as a set of benchmark data to check the accuracy of other calculations. Note that both OMP calculations (as well as many others) used a simple Hartree-Fock approximation for the static potential. We suggest that this is insufficient in the case of Ca, where there is strong mixing between the $4s^2$ and $4p^2$ configurations, and the 4s orbital itself is strongly affected by the $3p^6$ core polarization.

## B. Excitation cross sections

Figure 3 shows the angle-integrated cross section for electron-impact excitation of the $4s^2$ $^1S \rightarrow 4s4p$ $^1P^o$ resonance transition as a function of the incident electron energy. The experimental points were obtained by integration of the angle-differential measurements of Milisavljevic et al. [9]. From the available calculations we present only the most recent and most extensive calculations in the BSR-39 model [12], the present pseudostate BSR-483 model, and the CCC results [13], which also include the effect of the target continuum. Comparison of the two sets of BSR results with the same spectroscopic target wave functions allows us to assess the influence of the target continuum, whereas the comparison with the entirely independent CCC predictions provides an estimate for the uncertainty in the theoretical data. From this comparison we conclude that the target continuum has a noticeable influence even for this strong resonance transition, reducing the cross section at the maximum by $\sim 20\%$ and bringing the calculations into closer agreement with experiment. Some disagreement remains at 60 eV, but the experimental point seems low (see also Fig. 4 to be discussed next). The small differences between the BSR and CCC results is most likely due to the different target wave functions used in these calculations.

Figure 4 compares the apparent cross section for the $4s4p$ $^1P^o \rightarrow 4s^2$ $^1S$ spectral line as a function of the incident electron energy. Our BSR results are compared with the experimental data of Ehlers and Gallagher [8] and the CCC calculations of Fursa and Bray [13]. The apparent cross sections include cascade contributions from higher-lying states that may populate the radiating state. The contribution in this case is relatively small, not exceeding 15%. Inclusion of the target continuum again improves the agreement with experiment, and we estimate the overall uncertainty of the theoretical cross sections to be about 5%. This illustrates the accuracy that can be achieved by modern CCC or BSR codes for light quasi-two-electron atoms.

Angle-differential cross sections for electron-impact excitation of the $4s^2$ $^1S \rightarrow 4s4p$ $^1P^o$ resonance transition are presented in Fig. 5. We see very close agreement between the BSR-39 and BSR-483 results for a wide range of scattering angles. We conclude that the target continuum has a negligible influence on the angular dependence
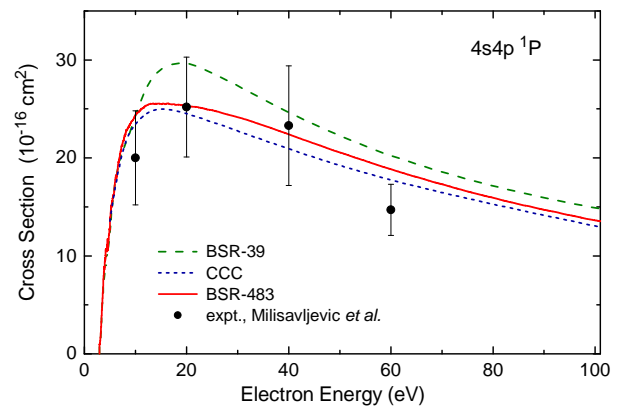
FIG. 3: Angle-integrated cross section for electron-impact excitation of the $4s^2$ $^1S \rightarrow 4s4p$ $^1P^o$ resonance transition as a function of the incident electron energy. Our BSR results are compared with the experimental data of Milisavljevic et al. [9] and CCC calculations of Fursa and Bray [13].
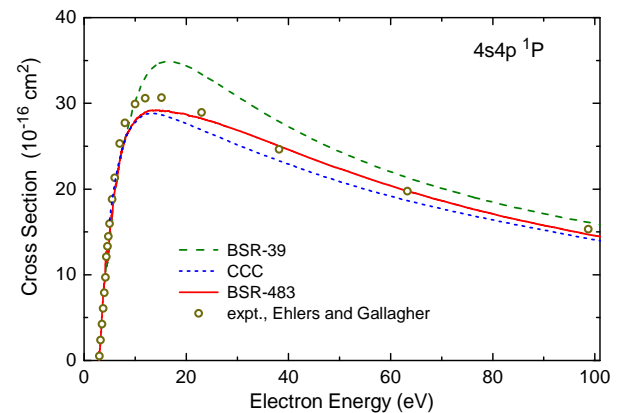
FIG. 4: Apparent cross section for the $4s4p$ $^1P^o \rightarrow 4s^2$ $^1S$ spectral line as a function of the incident electron energy. Our BSR results are compared with the experimental data of Ehlers and Gallagher [8] and CCC calculations of Fursa and Bray [13].

of the DCS as a function of scattering angle. This conclusion is similar to that drawn for the elastic DCS discussed above. The difference in the angle-integrated cross sections comes mainly from the small-angle regime, where the cross section rapidly changes by orders of magnitude. Except at 40 eV, there is also close agreement with the experimental shape of the DCS curve. Together with the close agreement between the CCC and BSR results at 10 and 20 eV, the comparison confirms the high accuracy of the present results, which we consider converged for all current practical purposes.

Figure 6 exhibits a sample of results for excitation of different target states from the ground state. The examples include different types of transitions, such as spin-forbidden exchange transitions as well as monopole, dipole, and quadrupole transitions to states with the
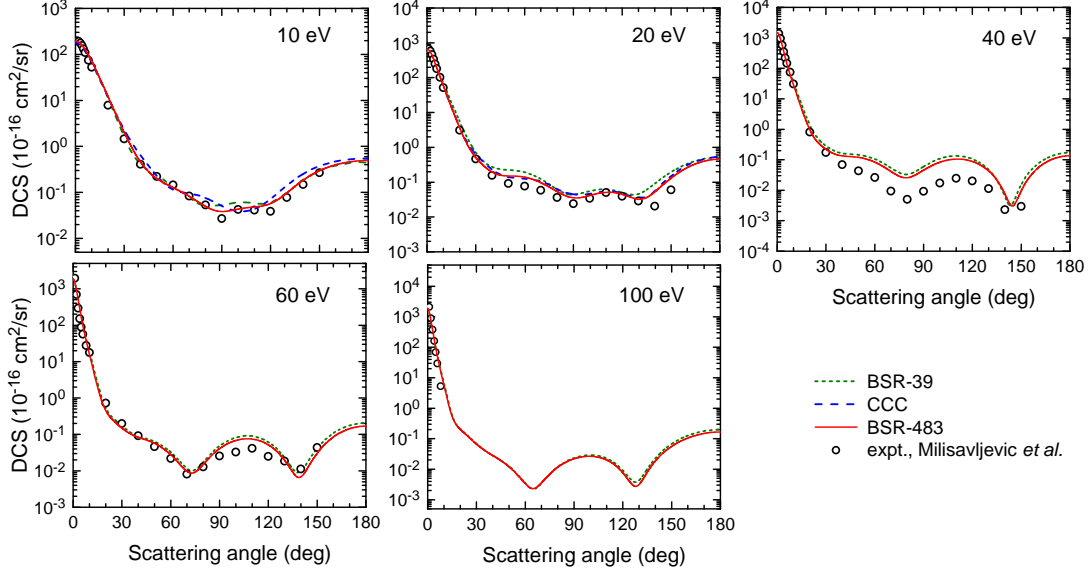
FIG. 5: Angle-differential cross sections for electron-impact excitation of the $4s^2\ ^1S \rightarrow 4s4p\ ^1P^o$ resonance transition from calcium atoms for incident electron energies of 10, 20, 40, 60 and 100 eV. Our BSR results are compared with the experimental data of Milisavljevic *et al.* [7], as well as with CCC calculations of Fursa and Bray [13].
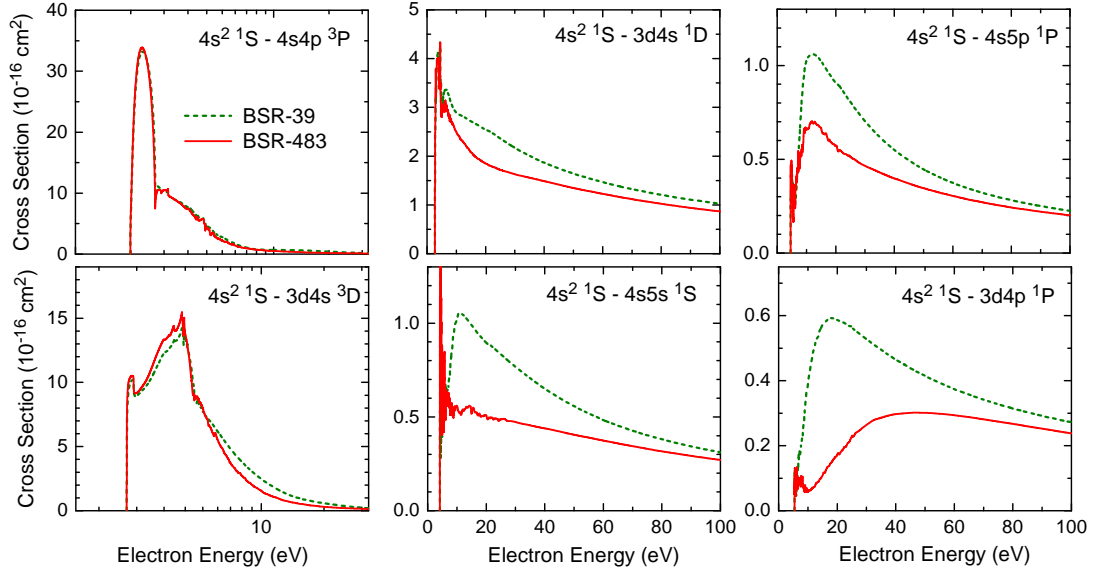


FIG. 6: Cross sections, as a function of collision energy, for electron-impact excitation of the selected states of calcium from the $4s^2\ ^1S$ ground state.

same total spin. As a general trend, results for the exchange transitions converge quickly due to the short-range interaction, and they do not depend very much on the scattering model. Note that the exchange transitions to the $3d4s\ ^3D$ and $4s4p\ ^3P^o$ states shown in the figure are intense, and near threshold their cross sections are comparable in magnitude with those for the resonant dipole transition to the $4s4p\ ^1P^o$ state. All spin-allowed transitions show a large influence of the target continuum, which decreases the cross sections in the main near-

threshold maximum. As expected, these corrections are most prominent for weak two-electron transitions, such as $4s^2\ ^1S - 3d4p\ ^1P^o$, where the target continuum corrections reach a factor of up to three and the peak energy is shifted significantly.

The same conclusions hold for transitions between excited states, which are shown in Fig. 7. There are only very few other results at intermediate energies available for comparison. We believe that all the predicted cross sections from our large-scale BSR-483 model (including
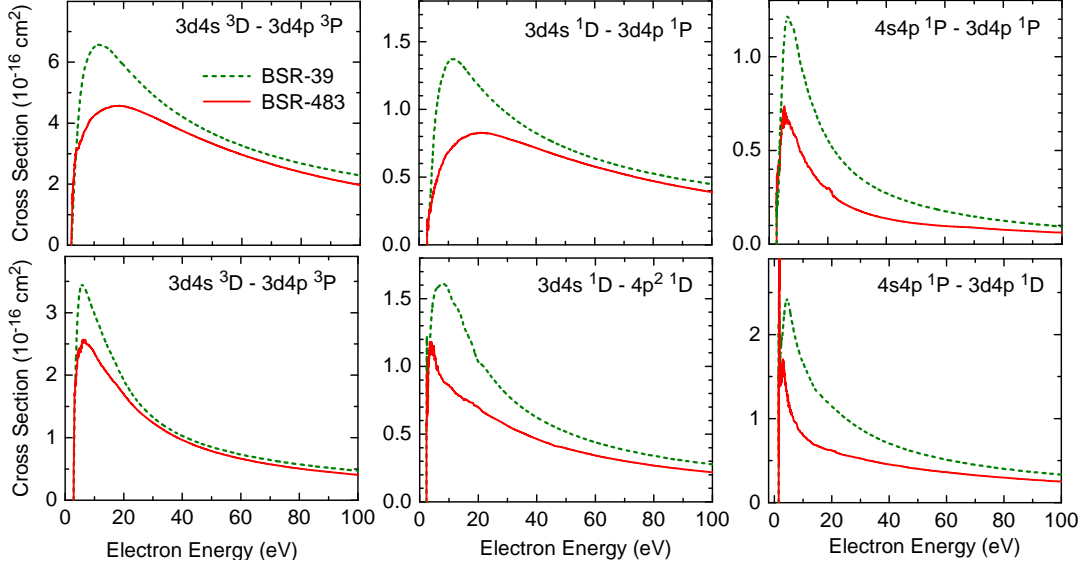
FIG. 7: Cross sections, as a function of collision energy, for electron-induced transitions from selected excited states of atomic calcium.

those for transitions between excited states) are close to convergence, but either experimental data or other independent calculations are needed for a reliable estimate of potentially remaining uncertainties. For all calculated transitions, we expect the same level of accuracy as for elastic scattering and the resonance transition discussed above.

### C. Ionization cross sections

The pseudostate approach also allows to generate ionization cross sections, as the summation of all excitations to the continuum pseudostates. Our ionization cross section is shown in Fig. 8. The comparison with experiment is complicated here due to the fact that existing absolute measurements were done for total ionization, where contributions of double ionization and inner-shell excitations are significant. Our BSR-483 model only allows the consideration of direct $4s$-ionization. For comparison with the measurements, we also added the excitation-autoionization contribution from the $3p$ subshell. This contribution was obtained in separate calculations of the $3p$ excitation to the core-excited $3p^5 3d 4s^2$ states, assuming that the strong dipole $3p - 3d$ transitions provide the main contribution to this process. As seen from Fig. 8, there is a good agreement with the relative measurements for single ionization reported by Okudaira [30], who used mass spectroscopy to select different ionization stages. These data were normalized to our cross sections at 90 eV. Comparison with the absolute measurements by Okuno [31] and Vainshtein et al. [32] for total ionization of Ca suggests that our calculations may slightly underestimate the cross section at low impact energies.
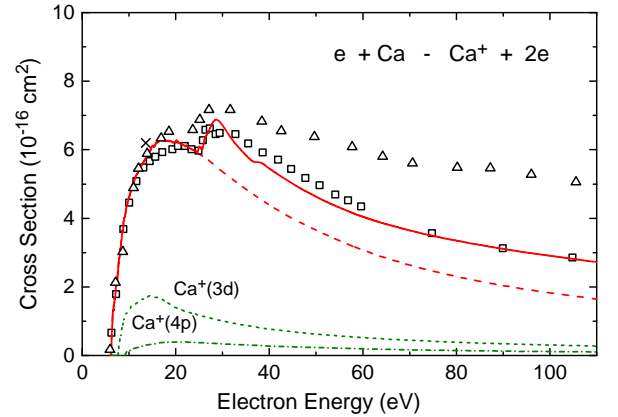


FIG. 8: Electron-impact ionization cross section for the ground state of calcium. Measurements: squares, Okudaira [30] (relative, visually normalized to the calculation); crosses, Okuno [31], triangles, Vainshtein et al. [32]. Dashed line - BSR-483 results for the direct $4s$ ionization, solid line - plus $3p$-excitation. Also shown are results for ionization-excitation to the $3p^6 3d$ and $3p^6 4p$ states of $Ca^+$.

We estimate the overall uncertainties of our cross sections for the single ionization of Ca to be about 10%.

Our pseudostates approach, together with the projection technique to select different final ionic states [33], is also able to consider the ionization + excitation process. As an example, Fig. 8 also presents the ionization-excitation cross sections to the $3p^6 3d$ and $3p^6 4p$ states of $Ca^+$. These pathways yield relatively small contributions to the total ionization, and ionization-excitation to other excited states of Ca+ was found to be negligible.
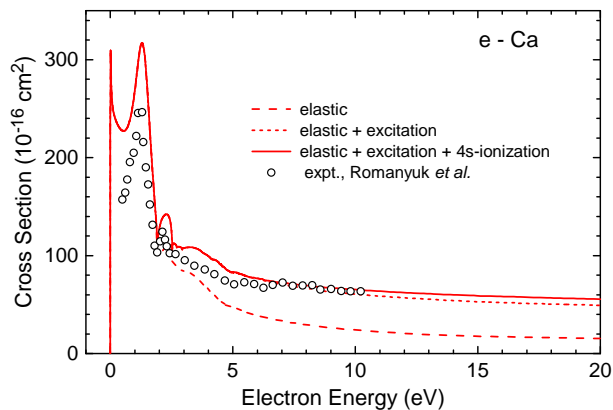
FIG. 9: Elastic, elastic + excitation, and grand total cross section for electron collisions with atomic calcium in the ground state, as obtained in the BSR-483 model. Also shown are the experimental data of Romanyuk *et al.* [34].

## D.   Grand-total cross sections from ground states

Our last comparison in Fig. 9 shows the grand total cross section for electron collisions with calcium atoms in their $4s^2$ $^1S$ ground state. This is the sum of the angle-integrated elastic, excitation, and ionization cross sections. While the elastic cross section provides the largest contribution at low energies, the contribution from excitation channels becomes dominant already at energies above 5 eV. The ionization processes never contribute more than 10% to the grand total cross section. Note that the relative contribution of the elastic, excitation, and ionization processes widely change from target to target. In fact, ionization often dominates at higher energies. We found such situations, for example, for electron scattering from atoms with an open $p$-shell.

There is a strong $d$-wave shape resonance at low energies, which was the subject our previous calculation [6] in the BSR-39 model. The present calculations in the pseudostate approach, BSR-483, confirm the previous results and conclusions. Except for very small energies, where the experimental resolution may become a factor, there is also generally good agreement in both the energy dependence and the magnitude of the grand total cross section with the absolute measurements by Romanyuk *et al.* [34].

## IV.   SUMMARY

We have carried out a detailed study of electron collisions with neutral calcium, including elastic scattering, excitation, and ionization processes from the ground and several excited states. State-to-state excitation cross sections were obtained for all transitions between the lowest 39 states of calcium. We expect the cross sections presented here to be useful for many practical applications. While only a small number of selected results could be presented in this paper, the entire dataset is available in electronic form upon request.

The calculations were performed with the BSR code [20]. The particular advantage of the approach is the possibility to employ term-dependent nonorthogonal one-electron orbitals in the description of the target states. This feature greatly improves the accuracy of the target description. In particular, the present target wave functions contain, fully *ab initio*, both valence and core-valence correlations, along with the relaxation effects due to the significant penetration of the $3d$ electron into the core.

The emphasis in the present calculations was placed on exploring the influence of coupling to the target continuum. The differences between the results from the BSR-39 and BSR-483 models provide an indication regarding the convergence of the close-coupling expansion for the problem at hand. Overall, the influence of the target continuum was found to be significant for most excitation cross sections, including even the strong resonance transition to the $4s4p$ $^1P^o$ state, where coupling to the target continuum improved the agreement with the available experimental data for the angle-integrated cross sections. At the same time, the target continuum has a negligible influence on elastic scattering and on the angular dependence (not the magnitude) of the differential cross sections, for both excitation and elastic scattering. We also showed that the present close-coupling calculations yield much closer agreement with the available measurements than all previous calculations using a model-potential approach.

Our pseudostate model, BSR-483, was also used to calculate the electron-impact direct ionization cross section for the calcium ground state. This fully nonperturbative calculation achieved good agreement with available experimental results for the single ionization cross sections of Ca. The excitation-autoionization contribution for ground-state ionization was also found to be important. Finally, the grand total cross section from the ground state, together with the contributions from elastic scattering, excitation, and ionization, was presented. We found large contributions from the excitation channels to the total cross section at intermediate energies.

[1] P. S. Barklem, Astron Astrophys Rev **24** (2016) 9.

[2] H. Holweger, Solar. Phys. **25** (1972) 14.

[3] P. Thoren, Astron. Astrophys. **358** (2000) L21.

[4] Y. Chmielewski, Astron. Astrophys. **353** (2000) 666.

[5] Christlieb, N., Gustafsson, B., Korn, A. J., et al. ApJ, **603** (2004) 708.

[6] O. Zatsarinny, K. Bartschat, S. Gedeon, V. Gedeon, and V. Lazur, Phys. Rev. A **74** (2006) 052708.

[7] S. Milisavljevic, D. Sevic, R. K. Chauhan, V. Pejcev, D. M. Filipovic, R. Srivastava, and B. P. Marinkovic, J. Phys. B **38** (2005) 2371.

[8] V. J. Ehlers and A. Gallagher, Phys. Rev. A **7**, 1573 (1973); *erratum:* Phys. Rev. A **9** (1974) 1026.

[9] S. Milisavljevic, D. Sevic, V. Pejcev, D.M. Filipovic, and B.P. Marinkovic, J. Phys. B **37** (2004) 3571.

[10] R. K. Chauhan, R. Srivastava, and A. D. Stauffer, J. Phys. B **38** (2005) 2385.

[11] S. Kawazoe T. Kai, R. K. Chauhan, R. Srivastava, and S. Nakazaki, J. Phys. B **39** (2006) 493.

[12] O. Zatsarinny, K. Bartschat, L. Bandurina, and S. Gedeon, J. Phys. B **40** (2007) 4023.

[13] D. V. Fursa and I. Bray, J. Phys. B **41** (2008) 145206.

[14] I. I. Shafranyoshy, T. A. Snegurskaya, N. A. Margitich, S. P. Bogacheva, V. I. Lengyel, and O. I. Zatsarinny, J. Phys. B **30** (1997) 2261.

[15] K. Muktavat, R. Srivastava, and A. D. Stauffer, J. Phys. B **35** (2002 4797).

[16] A. M. Samson and K. A. Berrington, At. Data Nucl. Data Tables **77** (2001) 87.

[17] O. Zatsarinny, K. Bartschat, D. V. Fursa, and I. Bray, J. Phys. B **49** (2016) 235701.

[18] P. S. Barklem, Y. Osorio, D. V. Fursa, I. Bray, O. Zatsarinny, K. Bartschat, and A. Jerkstrand, A&A **606** (2017) A11.

[19] O. Zatsarinny and K. Bartschat, J. Phys. B **46** (2013) 112001.

[20] O. Zatsarinny, Comp. Phys. Commun. **174** (2006) 273.

[21] D. Cvejanovic and A. J. Murray, J. Phys. B **36** (2003) 3591.

[22] O. Zatsarinny and C. Froese Fischer, Comp. Phys. Commun. **180** (2009) 2041.

[23] http://physics.nist.gov/cgi-bin/AtData.

[24] C. Froese Fischer and T. Tachiev, Phys. Rev. A **68** (2003) 012507.

[25] N. R. Badnell, J. Phys. B **32**, 5583 (1999); see also *http : //amdpp.phys.strath.ac.uk/UK_RmaX/codes.html*.

[26] V. M. Burke and M. J. Seaton, J. Phys. B **19** (1986) L527.

[27] S. P. Khare, A. Kumar, S. Vijay Shri, J. Phys. B **18** (1985) 1827.

[28] V. A. Kelemen, E. Yu. Remeta, and E. P. Sabad, J. Phys. B **28** (1995) 1527.

[29] D. Raj and A. Kumar, J. Phys. B **40** (2007) 3101.

[30] S. Okudaira, J. Phys. Soc. Japan **29** (1970) 409.

[31] Y. Okuno, J. Phys. Soc. Japan **31** (1971) 1189.

[32] L. A. Vainshtein, V. I. Ochkur, V. I. Rakhovskii, and A. M. Stepanov, Sov. Phys. JETP **34** (1972) 271.

[33] O. Zatsarinny and K. Bartschat, Phys. Rev. Lett. **107** (2011) 023203.

[34] N. I. Romanyuk, O. B. Shpenik, F. F. Papp, I. V. Chernysheva, I. A. Mandi, V. A. Kelemen, E. P. Sabad, and E. Yu. Remeta, Ukr. Fiz. Zh. **37** (1992) 1639.